C.E.D. Riboldi
On the Optimal Tuning of Individual Pitch Control for Horizontal-Axis Wind Turbines
Wind Engineering, Vol. 40, N. 4, 2016, p. 398-416
doi:10.1177/0309524X16651545

Wind Engineering
XX(X):1–28

DOI: 10.1177/ToBeAssigned
www.sagepub.com/
SAGE

On the optimal tuning of individual pitch control for horizontal axis wind turbines

Carlo E.D. Riboldi[1]

Abstract

Individual pitch control (IPC) has proved capable of reducing loads on the blades and shaft of horizontal axis wind turbines, at the price of a potentially substantial increase in actuator activity. With an accurate tuning of the control parameters the overall performance can be satisfactorily balanced, but a manual tuning procedure proves often unbearably costly and the solution found may be far from optimal. The present research tries to explore the feasibility of an optimal approach to the problem of tuning of IPC, by mapping reasonable cost functions with respect to some parameters of interest in control design. The analysis is carried out considering a possible IPC implementation, tested in virtual environment on a realistic testbed. The merit functions are analyzed also visually, in order to easily understand the effects of the various design parameters on the positions and quality of the respective optima. In a later stage, results of complete optimization runs are presented, and the approach is critically discussed.

Keywords

Individual pitch control (IPC), Control parameters, Optimization, Optimal tuning, Horizontal axis wind turbine

Introduction

In recent years much attention has been devoted to the reduction of fatigue loads by means of individual pitch control (IPC), as demonstrated by the rich literature dedicated

[1]Department of Aerospace Science and Technology, Politecnico di Milano, Italy

Corresponding author:
Carlo E.D. Riboldi, Ph.D.
Department of Aerospace Science and Technology, Politecnico di Milano
via La Masa 34, 20156 Milano, Italy
Email: carlo.riboldi@polimi.it

to the subject (see for instance Stol (2003), Stol and Balas (2003), Bossanyi (2003a), Bossanyi (2003b), Bossanyi (2004), Bossanyi (2005), van Engelen (2006), Geyler and Caselitz (2007), Geyler and Caselitz (2008), van Engelen and Kanev (2009), Leithead et al. (2009) and Bottasso et al. (2013)). Notwithstanding the extensive analysis of the topic, and the relevant advantage this control can provide on loads, IPC has not been generally adopted by industry, due to the potentially excessive workload imposed on pitch actuators, reflected in an increased value of the actuator duty cycle (ADC) with respect to what is obtained operating with a reference collective control.

The need to limit the action of pitch actuators without renouncing to the mitigating effect on loads provided by IPC can be dealt with by a proper tuning of the parameters of the IPC control law, mainly the proportional and integral gains for a model–free approach (Bossanyi (2003a)), or an array of control and load weights in the case of model–based control laws (Bottasso et al. (2013)). Control tuning is the result of a trade–off analysis and is usually carried out by means of a time–consuming manual procedure. In Bottasso et al. (2014) the use of IPC is restricted to a limited range of wind speeds, selected in order to maximize the effectiveness of control while minimizing actuator use. Yet also in that case, the selection of the activation range is completed by a manual trial and error procedure.

The issue represented by the need to contain the workload imposed on actuators while effectively reducing loads without going through a lengthy manual tuning procedure, can be addressed by selecting an optimal approach for determining the tuning parameters. A similar approach has been successfully tried for setting the parameters of a control law for turbine trimming (Bottasso et al. (2005)).

This work explores the effect of some relevant tuning parameters for a realistic IPC control law on a choice of possible merit functions. The analysis of the merit functions will be carried out considering test scenarios of increasing complexity. An approach by sub–problems is proposed, where the optimum of a merit function with respect to two optimization parameters at most is searched for, in order to allow mapping the merit function visually. This favors an easier observation of the effects of changing the values of the parameters of interest on the selected merit function and on its optimum.

It should be underlined that the main focus of the work is not on optimizing the control parameters, but mainly on understanding what is a good way to set up the problem of optimization based on such parameters. With this in mind, part of the paper is devoted to the analysis of the general behavior of the proposed merit functions with respect to changes in the balance of the quantities accounted for in their definition, i.e. measures of loads and ADC.

The outcome of the present work is primarily that of establishing whether an optimal approach to control tuning is feasible and it can be of help to engineers, providing a way to almost automatically select the values that control parameters should assume to optimize a comprehensive measure of performance, and secondarily that of providing some elements for determining what control design parameters and what testing scenarios should be taken into account in an optimal approach to the problem of control tuning. Finally, in case no optization tool was available in the tuning phase, this paper provides indications on how to reasonably tune the considered parameters.

The paper is organized as follows. In a first section it briefly presents the IPC architecture chosen for the analysis. The central section is devoted to the presentation of the considered scenarios of analysis. In the section devoted to the results, diagrams of the cost functions obtained in several different cases considered for this study are presented and commented. Next the results of some full optimization runs are shown, supporting what can be concluded from the preliminary analysis of the cost functions. Finally, a summary of the results and some critical considerations are presented in the closing paragraph.

Individual pitch control law

As recalled in the introduction, there are multiple ways to implement an IPC, witnessed by the wide literature on the topic. A model–free IPC similar to that proposed by Bossanyi in Bossanyi (2005) was selected for this analysis due to its greater simplicity with respect to other implementations. A difference between the adopted control scheme with respect to that presented in the works of Bossanyi is the use of both out–of–plane and in–plane blade load signal instead of out–of–plane only (Riboldi (2012)). The main features of the adopted implementation will be outlined in this paragraph.

The IPC law takes as input the out–of–plane and in–plane bending moments at the root of the blades, $\boldsymbol{M}_{\mathrm{OoP}} = \{M_{\mathrm{OoP},1}, M_{\mathrm{OoP},2}, M_{\mathrm{OoP},3}\}^T$ and $\boldsymbol{M}_{\mathrm{InP}} = \{M_{\mathrm{InP},1}, M_{\mathrm{InP},2}, M_{\mathrm{InP},3}\}^T$ respectively for a three–bladed turbine. These are transformed by means of the 1–per–rev (1P) Coleman's transform into two fixed frame equivalent loads (van Engelen (2006))

$$\boldsymbol{M}_{d-q} = \left\{ \begin{array}{c} \boldsymbol{M}_d \\ \boldsymbol{M}_q \end{array} \right\} = \boldsymbol{C}_{\mathrm{OoP}}(\Psi)\boldsymbol{M}_{\mathrm{OoP}} + \boldsymbol{C}_{\mathrm{InP}}(\Psi)\boldsymbol{M}_{\mathrm{InP}} \tag{1}$$

where Ψ represents the azimuth of the rotor, measured as that of the first blade. The two transform matrices in Eq. 1 are defined as

$$\begin{aligned} \boldsymbol{C}_{\mathrm{OoP}}(\Psi) &= \left[\begin{array}{ccc} \cos(\Psi) & \cos(\Psi + \frac{2\pi}{3}) & \cos(\Psi + \frac{4\pi}{3}) \\ \sin(\Psi) & \sin(\Psi + \frac{2\pi}{3}) & \sin(\Psi + \frac{4\pi}{3}) \end{array} \right] \\ \boldsymbol{C}_{\mathrm{InP}}(\Psi) &= \sin(\gamma) \left[\begin{array}{ccc} -\sin(\Psi) & -\sin(\Psi + \frac{2\pi}{3}) & -\sin(\Psi + \frac{4\pi}{3}) \\ \cos(\Psi) & \cos(\Psi + \frac{2\pi}{3}) & \cos(\Psi + \frac{4\pi}{3}) \end{array} \right] \end{aligned} \tag{2}$$

where the angle γ is the cone angle of the rotor, considered positive when bending the blades towards the upwind direction.

The $\boldsymbol{M}_{d-q}$ signals in Eq. 1 are subsequently fed to two decoupled proportional–integral (PI) loops producing two control signals in the fixed frame

$$\left\{ \begin{array}{c} \beta_d \\ \beta_q \end{array} \right\} = \boldsymbol{k}_P \boldsymbol{M}_{d-q} + \boldsymbol{k}_I \int_0^t \boldsymbol{M}_{d-q} \mathrm{d}\tau \tag{3}$$

where $\boldsymbol{k}_P$ and $\boldsymbol{k}_I$ are 2–by–2 diagonal gain matrices.

The resulting β_d and β_q control signals are transformed back into time domain using the inverse Coleman's transform, yielding

$$\left\{ \begin{array}{c} \Delta\beta_1 \\ \Delta\beta_2 \\ \Delta\beta_3 \end{array} \right\} = \boldsymbol{C}^*(\Psi) \left\{ \begin{array}{c} \beta_d \\ \beta_q \end{array} \right\} \tag{4}$$

where the matrix representing the inverse transformation is

$$\boldsymbol{C}^*(\Psi) = \left[\begin{array}{cc} \cos(\Psi) & \sin(\Psi) \\ \cos(\Psi + \frac{2\pi}{3}) & \sin(\Psi + \frac{2\pi}{3}) \\ \cos(\Psi + \frac{4\pi}{3}) & \sin(\Psi + \frac{4\pi}{3}) \end{array} \right]. \tag{5}$$

The $\Delta\beta_i$, $i = 1, 2, 3$ pitch control signals obtained from Eq. 4, which sum up to zero at every time step by constitution, can be added to the pitch value β_c coming from a collective controller used for trimming the machine to the correct rotor speed and power output in a multi–layer fashion as explained in Riboldi (2012) and Bottasso et al. (2013), yielding

$$\beta_i = \beta_c + \Delta\beta_i, \quad i = 1, 2, 3. \tag{6}$$

As suggested in van Engelen (2006), in order to avoid the generation of spurious control signals at frequencies higher than the 1P, the load signals are low–pass filtered in order to let only frequencies up to the 1P be fed to Coleman's transform.

The gain coefficients for this IPC law are four in principle (two for each matrix $\boldsymbol{k}_P$ and $\boldsymbol{k}_I$), but as suggested by practice the controller produces usually satisfying results when considering the same gains for the two decoupled loops (Riboldi (2012); Bottasso et al. (2013, 2014)). This simplifies tuning, allowing to set the number of scalar control design parameters to two for this control law, thus assuming a gain structure like $\boldsymbol{k}_P = k_P \cdot \boldsymbol{I}$ and $\boldsymbol{k}_I = k_I \cdot \boldsymbol{I}$, where $\boldsymbol{I}$ is a 2–by–2 identity matrix.

In order to limit the increase in ADC due to IPC activity a logic for conditional activation of IPC has been implemented, where the triggering variable is the speed of the air stream $U_0(t)$ as measured by an anemometer on top of the tower (Bottasso et al. (2014)). The number of activation ranges, i.e. intervals of wind speed values for which the IPC is active, has been set to two, where the first can be centered at the rated wind speed U_r and the second at the cut–out U_o. The IPC is activated when the wind speed $U_0(t)$ measured by the anemometer is such that

$$U_{0,\,r} - \frac{R_r}{2} \leq U_0(t) \leq U_{0,\,r} + \frac{R_r}{2} \cup U_{0,\,o} - \frac{R_o}{2} \leq U_0(t) \leq U_{0,\,o} + \frac{R_o}{2}. \tag{7}$$

Due to their predictably relevant impact on ADC and load performance indices, the amplitudes R_r and R_o of the two activation ranges have been investigated as tuning parameters for the control law, besides the gains k_P and k_I. The effect of such parameters will be presented in detail in the section dedicated to the results.

The frequent activation and deactivation of IPC consequent to a time–varying wind speed, as it is typical in turbulence, may generate frequent and unwanted local peak

loads, in turn raising fatigue. In order to minimize this effect, two countermeasures have been adopted. Firstly, a smooth control activation and deactivation procedure has been implemented. According to such procedure the controller gains are brought from zero to their design values and viceversa for activation and deactivation respectively following a linear–in–time law. The switch–on/off procedure is triggered whenever the wind speed is entering or leaving an operational range. Secondarily, in order to avoid frequent activations or deactivations especially when working close to one of the boundaries of the operational ranges, the wind speed signal coming from the sensor at the top of the tower is low–pass filtered with a moving average filter with an appropriate averaging window of the order of some seconds. The duration of the activation and deactivation procedures can be set according to necessity and can be of the order of a few seconds.

Finally, practice suggests that the action of individual pitch control should be limited when the machine is operating in the region close to the rated wind speed, where the trimmer typically passes from controlling through torque only (partial power regions II and $\text{II}^{\frac{1}{2}}$), due to the blades working in proximity of a hard minimum pitch limit, to a condition where pitch is free to move and both pitch and torque control are usually active for trimming (full power region III). In order to avoid interference in the basic trimming action from the superimposed IPC control component (Bottasso et al. (2013)), the action of the latter is depressed by multiplying the value of the gains k_P and k_I by a factor $\zeta < 1$ when the machine is operated in such critical region.

Build–up of merit functions

The action of IPC bears usually visible reductions on the 1P frequency components of the target loads, i.e. the out–of–plane and in–plane moments $\boldsymbol{M}_{\text{OoP}}$ and $\boldsymbol{M}_{\text{InP}}$ at the root of the blades, with respect to what is obtained when only the trimmer is controlling the machine (Bossanyi (2003a,b)). As a matter of fact, thanks to the relationship between those blade loads and the $\boldsymbol{M}_{d-q}$ moments expressed by Coleman's transform (Eq. 1), a reduction of the constant component of the nodding and yawing bending moments measured on a cross–section of the shaft in a fixed system $\boldsymbol{M}_s = \{M_{\text{yaw}}, M_{\text{nod}}\}^T$ (Bossanyi (2004)) is reflected in a reduction in the 1P amplitude of blade loads measured in the rotating system. The moments $\boldsymbol{M}_s$ are not defined exactly as $\boldsymbol{M}_{d-q}$, due at least to the fact the the actual nodding and yawing moment are affected also by the moment bound to total shear forces at the roots of the blades. However, the values in $\boldsymbol{M}_{d-q}$ and $\boldsymbol{M}_s$ are related and usually proportional (Riboldi (2012)).

Ideal constant wind conditions

The theory of individual pitch control is mainly developed under ideal, strictly time–periodic conditions (Bossanyi (2004); van Engelen and Kanev (2009); Bottasso et al. (2013)). For this reason, a first performance assessment of IPC laws should be carried out in ideal constant wind conditions, generating fully periodic time signals in the response of the machine, due to shear and gravity effects. Advantages in the values of loads are usually clearly visible in such scenario in the form of a reduction of the peak–to–peak amplitude in the time histories of the blade moments, dominated by

the 1P (Riboldi (2012); Bottasso et al. (2013)). The peak–to–peak amplitude at the 1P frequency, indicated as Δ^{1P}_{p-p}, can be obtained for a generic signal expressed as a function of the azimuth $s = s(\Psi)$. It can be computed demodulating the signal at the 1P frequency (Riboldi (2012)). Considering a demodulation over one rotor revolution, the amplitude of the 1P component in the signal s can be defined in analytical terms as

$$A^{1P}_{s,\sin} = \frac{1}{\pi}\int_{\Psi-2\pi}^{\Psi} s(\psi)\sin(\psi)\mathrm{d}\psi, \quad A^{1P}_{s,\cos} = \frac{1}{\pi}\int_{\Psi-2\pi}^{\Psi} s(\psi)\cos(\psi)\mathrm{d}\psi$$
$$A^{1P}_{s} = \sqrt{{A^{1P}_{s,\sin}}^2 + {A^{1P}_{s,\cos}}^2} \tag{8}$$

so that the peak–to–peak difference at the 1P is $\Delta^{1P}_{p-p}s = 2A^{1P}_s$. Considering all three blades, the average of the peak–to–peak can be written as

$$\widetilde{\Delta}^{1P}_{p-p}\boldsymbol{M}_{\mathrm{OoP}} = \frac{1}{3}\sum_{i=1}^{3}\Delta^{1P}_{p-p}(\boldsymbol{M}_{\mathrm{OoP},i}), \quad \widetilde{\Delta}^{1P}_{p-p}\boldsymbol{M}_{\mathrm{InP}} = \frac{1}{3}\sum_{i=1}^{3}\Delta^{1P}_{p-p}(\boldsymbol{M}_{\mathrm{InP},i}) \tag{9}$$

where the symbol $\widetilde{(\cdot)}$ denotes an average over the three blades.

It is noteworthy that the computation of the amplitude corresponding to an assigned harmonic component can be performed with the azimuth–based method highlighted in Eq. 8 also when the signal is not periodic in time. However, the amplitude corresponding to a certain frequency in the generic signal would clearly change in time in not ideal conditions, i.e. when the wind speed is changing in time as in turbulence. Hence peak–to–peak difference is of particular relevance only in ideal constant wind conditions, yielding a strictly periodic behavior of all load measures of interest.

Similarly to the blades, also the constant components of the nodding and yawing moments on a cross–section of the shaft are expected to be reduced by IPC in constant wind. They can be defined as

$$\overline{\boldsymbol{M}}_{\mathrm{nod}} = \frac{1}{t}\int_0^t M_{\mathrm{nod}}(\tau)\mathrm{d}\tau, \quad \overline{\boldsymbol{M}}_{\mathrm{yaw}} = \frac{1}{t}\int_0^t M_{\mathrm{yaw}}(\tau)\mathrm{d}\tau \tag{10}$$

where symbol $\overline{(\cdot)}$ denotes an average in time.

As previously stated, the advantage on selected loads comes at the price of an increased actuator duty cycle (ADC), reflecting a more conspicuous motion of pitch actuators. The definition of ADC_i adopted here for each blade is based on pitch rate (Stol (2003); Riboldi (2012)), yielding

$$\mathrm{ADC}_i = \frac{1}{t}\int_0^t |\dot{\beta}_i(\tau)|\mathrm{d}\tau, \quad i = 1,2,3 \tag{11}$$

where $\dot{(\cdot)}$ represents the time derivative. The average actuator duty cycle can be defined as $\widetilde{\mathrm{ADC}} = \frac{1}{3}\sum_{i=1}^{3}\mathrm{ADC}_i$.

A merit function allowing to simultaneously monitor both the expected increase in load performance and actuator motion in ideal constant wind conditions may be

based on average blade load peak–to–peak, shaft cross–sectional bending average and average ADC. In order to cover all operational regions, multiple constant wind turbine runs at a number $N_{U,\,c}$ of wind intensities $U_{0,\,j},\ j = 1, \ldots, N_{U,c}$ should be considered between cut–in and cut–out. For a proper scaling of a yet–to–be–defined merit function, the normalized values of these quantities should be preferred to the corresponding dimensional definition. Furthermore, in order to assure that the merit function be definite positive, it is necessary to take the absolute value of all quantities of interest. Therefore for the quantities defined in Eq. 9, 10, 11 the respective positive, normalized values can be defined as

$$\begin{aligned} \rho\left(\widetilde{\Delta}^{1P}_{p-p}\boldsymbol{M}_{\mathrm{OoP}}\right) &= \frac{\left|[\widetilde{\Delta}^{1P}_{p-p}\boldsymbol{M}_{\mathrm{OoP}}]_{\mathrm{IPC}}\right|}{\left|[\widetilde{\Delta}^{1P}_{p-p}\boldsymbol{M}_{\mathrm{OoP}}]_{\mathrm{ref}}\right|} \qquad \rho\left(\widetilde{\Delta}^{1P}_{p-p}\boldsymbol{M}_{\mathrm{InP}}\right) = \frac{\left|[\widetilde{\Delta}^{1P}_{p-p}\boldsymbol{M}_{\mathrm{InP}}]_{\mathrm{IPC}}\right|}{\left|[\widetilde{\Delta}^{1P}_{p-p}\boldsymbol{M}_{\mathrm{InP}}]_{\mathrm{ref}}\right|} \\ \rho\left(\overline{M}_{\mathrm{nod}}\right) &= \frac{\left|[\overline{M}_{\mathrm{nod}}]_{\mathrm{IPC}}\right|}{\left|[\overline{M}_{\mathrm{nod}}]_{\mathrm{ref}}\right|} \qquad \rho\left(\overline{M}_{\mathrm{yaw}}\right) = \frac{\left|[\overline{M}_{\mathrm{yaw}}]_{\mathrm{IPC}}\right|}{\left|[\overline{M}_{\mathrm{yaw}}]_{\mathrm{ref}}\right|} \\ \rho\left(\widetilde{\mathrm{ADC}}\right) &= \frac{\left|[\widetilde{\mathrm{ADC}}]_{\mathrm{IPC}}\right|}{\left|[\widetilde{\mathrm{ADC}}]^{*}_{\mathrm{ref}}\right|} \end{aligned} \tag{12}$$

where subscript $[\cdot]_{\mathrm{IPC}}$ indicates results obtained with IPC activated, whereas $[\cdot]_{\mathrm{ref}}$ indicates the reference condition where IPC is not active and only the trimmer is working to control the machine. Divisions are performed element by element on arrays, i.e. on the first line of Eq. 12. Note that $\widetilde{\mathrm{ADC}}$ is normalized with respect to $[\widetilde{\mathrm{ADC}}]^{*}_{\mathrm{ref}}$, defined as

$$[\widetilde{\mathrm{ADC}}]^{*}_{\mathrm{ref}} = \begin{cases} [\widetilde{\mathrm{ADC}}]_{\mathrm{ref}} & \text{if } [\widetilde{\mathrm{ADC}}]_{\mathrm{ref}} \neq 0 \\ \sigma > 0 & \text{if } [\widetilde{\mathrm{ADC}}]_{\mathrm{ref}} = 0 \end{cases} . \tag{13}$$

This is to avoid division by zero in the possible case of null reference $[\widetilde{\mathrm{ADC}}]_{\mathrm{ref}}$, that can be encountered for a very low wind speed U_0 in constant wind conditions when the trimmer is operating alone, usually at pitch for maximum power coefficient (partial power region II), due to the usually slight collective pitch activity in this region (Bottasso et al. (2012)). The value of σ may be set close to a typical value of $\widetilde{\mathrm{ADC}}$ encountered with IPC deactivated for the lower portion of full power region III, i.e. for those low wind speed values above the rated for which pitch control can move freely.

A well–tuned IPC law working in a constant wind scenario should lower all load indices in Eq. 12 except $\rho\left(\widetilde{\mathrm{ADC}}\right)$. Therefore, a possible synthetic measure of the overall performance of the IPC controller can take the form of the following merit function

$$\begin{aligned} J_c = \frac{1}{N_{U,\,c}} \sum_{j=1}^{N_{U,\,c}} \Big(& g_j \rho\left(\widetilde{\Delta}^{1P}_{p-p}\boldsymbol{M}_{\mathrm{OoP},j}\right) + h_j \rho\left(\widetilde{\Delta}^{1P}_{p-p}\boldsymbol{M}_{\mathrm{InP},j}\right) + \\ & + l_j \rho\left(\overline{M}_{\mathrm{nod},j}\right) + m_j \rho\left(\overline{M}_{\mathrm{yaw},j}\right) + a_j \rho\left(\widetilde{\mathrm{ADC}}_j\right)\Big) \end{aligned} \tag{14}$$

where g_j, h_j, l_j, m_j and a_j are positive scalar weights. Note that all components in J_c except $\rho\left(\widetilde{\mathrm{ADC}}_j\right)$ are expected to be lower than unity for increasing reasonable values of the gain multipliers k_P, k_I and of the operational ranges R_r and R_o, when IPC is working properly. Furthermore, the components of the merit function are all positive by definition. Therefore, J_c is definite positive, and the load and control indices in it tend to be respectively lowered and raised by a more intense control action, hence possibly producing a minimum for J_c.

Turbulent wind conditions

When moving to a turbulent wind scenario, the mitigating effect of IPC on loads can not be easily quantified studying the performance indices adopted for a constant wind scenario. In particular, in the new condition the change in the damage equivalent load (DEL) computed from turbulent time histories is more representative than the 1P peak–to–peak difference, due to the non–periodic time behavior of the load signals in turbulence.

The DEL can be computed using a standard rainflow technique, obtaining one load value equivalent to one time history (Riboldi (2012); Bottasso et al. (2013)). The DEL can be computed for both blade loads and shaft loads, and it will be indicated here with the operator $\Lambda = \mathrm{DEL}(\cdot)$. Consequently, load values relevant for the analysis in turbulence are $\Lambda M_{\mathrm{OoP},i}$, $\Lambda M_{\mathrm{InP},i}$, $i = 1, 2, 3$ for the blades, and ΛM_{nod}, ΛM_{yaw} for the shaft.

A significant reduction of the DEL on the blade roots and shaft cross–sectional bending loads can be expected from a well tuned IPC working in turbulence (Riboldi (2012); Bottasso et al. (2013)). Furthermore, the value of shaft cross–sectional bending moments averaged in time should decrease with respect to what is obtained from the baseline trimmer when IPC is activated (Bossanyi (2003a); Riboldi (2012); Bottasso et al. (2013)). Consequently, the quantities in Eq. 10 are of interest also for the turbulent wind scenario. Similarly, the definition of ADC in Eq. 11 adopted for the ideal case applies also to this scenario.

As for the ideal case, it is advisable to study normalized values of the quantities of interest instead of their actual values, in order to assess more directly whether the performance index is increasing or decreasing with respect to the baseline. Summarizing, the following set of performance indices can be considered in the case of the turbulent wind scenario

$$
\begin{aligned}
\rho\left(\widetilde{\Lambda}\boldsymbol{M}_{\mathrm{OoP}}\right) &= \frac{\left|[\widetilde{\Lambda}\boldsymbol{M}_{\mathrm{OoP}}]_{\mathrm{IPC}}\right|}{\left|[\widetilde{\Lambda}\boldsymbol{M}_{\mathrm{OoP}}]_{\mathrm{ref}}\right|} \qquad \rho\left(\widetilde{\Lambda}\boldsymbol{M}_{\mathrm{InP}}\right) = \frac{\left|[\widetilde{\Lambda}\boldsymbol{M}_{\mathrm{InP}}]_{\mathrm{IPC}}\right|}{\left|[\widetilde{\Lambda}\boldsymbol{M}_{\mathrm{InP}}]_{\mathrm{ref}}\right|} \\
\rho\left(\Lambda M_{\mathrm{nod}}\right) &= \frac{|[\Lambda M_{\mathrm{nod}}]_{\mathrm{IPC}}|}{|[\Lambda M_{\mathrm{nod}}]_{\mathrm{ref}}|} \qquad \rho\left(\Lambda M_{\mathrm{yaw}}\right) = \frac{|[\Lambda M_{\mathrm{yaw}}]_{\mathrm{IPC}}|}{|[\Lambda M_{\mathrm{yaw}}]_{\mathrm{ref}}|} \\
\rho\left(\overline{M}_{\mathrm{nod}}\right) &= \frac{\left|[\overline{M}_{\mathrm{nod}}]_{\mathrm{IPC}}\right|}{\left|[\overline{M}_{\mathrm{nod}}]_{\mathrm{ref}}\right|} \qquad \rho\left(\overline{M}_{\mathrm{yaw}}\right) = \frac{\left|[\overline{M}_{\mathrm{yaw}}]_{\mathrm{IPC}}\right|}{\left|[\overline{M}_{\mathrm{yaw}}]_{\mathrm{ref}}\right|}
\end{aligned}
\tag{15}
$$

$$\rho\left(\widetilde{\mathrm{ADC}}\right) = \frac{\left|\left[\widetilde{\mathrm{ADC}}\right]_{\mathrm{IPC}}\right|}{\left|\left[\widetilde{\mathrm{ADC}}\right]^{*}_{\mathrm{ref}}\right|}$$

where all quantities are ratioed with respect to a condition where the trimmer is operating alone, and $\left[\widetilde{\mathrm{ADC}}\right]^{*}_{\mathrm{ref}}$ is defined as in Eq. 13.

In order to measure the effect of IPC in turbulent conditions, considering an array of multiple $N_{U,\,t}$ time histories of wind with different average speed values, a merit function as in Eq. 16 can be formulated, based on the quantities in Eq. 15. This yields

$$\begin{aligned} J_t = \frac{1}{N_{U,\,t}} \sum_{j=1}^{N_{U,\,t}} \big(& p_j \rho\left(\Lambda \boldsymbol{M}_{\mathrm{OoP},j}\right) + q_j \rho\left(\Lambda \boldsymbol{M}_{\mathrm{InP},j}\right) + \\ & + r_j \rho\left(\Lambda M_{\mathrm{nod},j}\right) + s_j \rho\left(\Lambda M_{\mathrm{yaw},j}\right) + \\ & + l_j \rho\left(\overline{M}_{\mathrm{nod},j}\right) + m_j \rho\left(\overline{M}_{\mathrm{yaw},j}\right) + a_j \rho\left(\widetilde{\mathrm{ADC}}_j\right)\big) \end{aligned} \tag{16}$$

where p_j, q_j, r_j, s_j, l_j, m_j and a_j are positive scalar weights. Similarly to J_c, all components in J_t are positive, so that the merit function is definite positive. A good performance of the IPC control law should bring all load indices below unity, at the price of an increase in $\rho\left(\widetilde{\mathrm{ADC}}_j\right)$, which will be above unity. Furthermore, as it was the case for J_c, a more intense control action should lower the load indices while at the same time it should tend to increase pitch motion. Hence a minimum for J_t is likely to appear for a proper selection of the tuning parameters.

Management of weights

The weights in Eq. 14, 16 contribute to the shaping of the merit functions. In particular, the ratio between the weights attributed to the measures of load and to ADC can be set in order to make the positive effect of the former or the detrimental effect of the latter prevail in the overall value of the considered merit function.

Good practices for setting the values of the weights in merit functions in engineering problems are largely dependent on the specific problem itself, and they usually involve some arbitrary choices. In this case, two considerations led to the set up of guidelines for choosing the weights.

Firstly, what is known from industry is that the effect of ADC is reflected in major technical problems leading to premature consumption of actuators, and making major faults more likely, in turn lowering energy production over time due to an increased time required for machine servicing. This finally leads to an increase in costs. The attitude towards IPC shown by industry is consequently that of considering an increase in ADC as a particularly worrying effect of this control logic. On the other hand, as can be seen from many quantitative results in the literature (Stol (2003); Stol and Balas (2003); Bottasso et al. (2014)), the normalized increase in ADC can be more substantial than the normalized reduction of load indices, hence even with neutral (unitary) weights the attitude of the chosen merit functions is expected to feature a greater sensitivity to ADC than to the

other measures of performance. For this reason, lower values of a_j with respect to other weights should be imposed in the computation of J_c and J_t.

Secondarily, turbine certification standards (IEC61400-1 (2005)) promote the use of a Weibull distribution for analyzing performance indices depending on the wind speed. The effect of the adoption of the Weibull distribution in the computation of J_c and J_t has been tested by setting the weights in the merit functions in Eq. 14 and 16 to different values for the various average wind speeds of the corresponding simulations, scaling a starting value assigned by the user for each simulation according to a Weibull probability distribution. In analytical terms,

$$w_j = w_j^* \cdot W(\overline{U_{0,j}(t)}), \quad j = 1, ..., N_U \tag{17}$$

where w_j is the actual value of the weight, w_j^* the generic starting weight value not accounting for the effect of the Weibull scaling (possibly equal for all simulations), $W(U_0)$ is the Weibull function for the assigned certification class of the machine, and N_U the number of considered simulations.

Results

All results proposed in the following were obtained working on the `FAST` (Jonkman and Buhl (2005)) model of an existing onshore three–bladed, horizontal axis, upwind, 3.0 MW turbine. The flexible modes of blades, shaft and tower allowed by `FAST` have been enabled, providing for a sufficiently accurate analysis of the response of the machine in terms of deformation and loads. The model was preliminarily validated with respect to the more sophisticated multi–body/FEM code `Cp-Lambda` (Bauchau et al. (2003); Bottasso and Croce (2012)). The model has been coupled with an external controller, where the trimmer and IPC control laws have been implemented together with supervisory features for managing shut–on, shut–off and emergency procedures (Riboldi (2012)).

For the present analysis, a suitably tuned LQR has been used for trimming the machine in all operating regions (Riboldi (2012); Bottasso et al. (2012)). Being the innermost control layer, the trimmer is tasked with the regulation of power output, computing the torque and collective pitch inputs based on basic machine measures including the speed of the rotor (Riboldi (2012); Bottasso et al. (2012, 2013)). In order to cope with the different quality of the various wind speed regions of the operating envelope, a reduced model of the system has been linearized for several wind speeds between cut–in and cut–out, thus implementing a scheduling of the trimmer with respect to the wind. The minimum pitch value considered for trimming is slightly higher than the lower hard pitch limit of the machine, allowing the IPC signal, added to the collective control signal according to Eq. 6, to be actuated mostly free of hardware constraints even for low wind speeds in partial power region.

As this analysis is centered on the behavior of pitch control, the aero–elastic model of the wind turbine has been augmented with detailed second order models of the dynamics of pitch actuators. This assures a good fidelity to real field conditions, which is relevant especially when testing the controller in turbulence.

The analysis of the merit functions in Eq. 14 and 16 has been carried out through multiple simulation runs of the `FAST` model of the considered turbine in constant and turbulent wind respectively, with different settings of the IPC tuning parameters. The `FAST` simulation code was deemed sufficiently accurate for the proposed analysis, mainly centered on relative changes in blade and shaft loads, and it was selected also due to the need to launch a relatively large amount of simulations while containing the overall execution time of the simulation runs. As a matter of fact, the mapping of the merit functions may be comparatively computationally heavier than optimization in terms of execution time, so great care should be taken to contain the overall length of the mapping process, including the selection of a lighter simulator.

The chance to visually check the merit functions is of great importance for understanding what is the shape they assume. This can be guaranteed in principle only when simultaneously studying the effect of two parameters at most. For this reason, in order to privilege the ease of interpretation of the results of the analysis, it was decided to study the effect on the merit functions of separate sets of two parameters.

The results of the proposed approach to the optimal analysis by sub–problems will be compared to the outcome of more comprehensive optimization runs on more than two parameters together in a later subsection.

The first couple of parameters is that of the proportional and integral gains k_P and k_I. The second couple is that of R_r and R_o defining the ranges of activation of IPC. The effect of the first couple has been considered on both J_c and J_t, whereas the second only on J_t.

The reason for that, besides saving on the computational time and length of the paper, is the different aim of the study of the two proposed scenarios, and their respective merit functions. The ideal scenario, thanks to the relatively reduced simulation time and ease of analysis of the results, is that most frequently considered for the manual tuning of the IPC gains whatever the implementation (Stol (2003); Bossanyi (2004); Riboldi (2012)). Furthermore, in the ideal scenario the constant value of the characteristic multiples of the rev forcing frequency over time makes it easier to verify theoretical principles from control theory. On the other hand, moving to a more realistic turbulent scenario allows to verify the system in slightly off–design conditions, a step closer to the operating conditions found in real environment. By comparing the effect of gains in the ideal and turbulent wind scenarios and their respective merit functions some conclusions can be drawn about their relevance to the tuning procedure.

The need for implementing conditional activation arises from practical considerations bound to the excessive load on actuators and the reduction of the advantages provided by IPC in the field, i.e. far from ideal constant wind conditions (Bottasso et al. (2014)). For this reason it makes sense to check the effect of the characteristic ranges R_r and R_o mainly in turbulent wind conditions and on J_t, in order to see whether this technological solution improves the performance of IPC in more realistic conditions.

Effects of individual pitch control gains

Constant wind scenario For the constant wind scenario, for every set of assigned control design parameters, $N_{U,\,c} = 12$ simulations of 100 sec in constant wind have been carried out. The wind speeds adopted for these simulations are from the cut–in $U_{0,\,i} = 3$ m/sec to the cut–out $U_{0,\,o} = 25$ m/sec every 2 m/sec.

A square test grid has been considered, based on values of the proportional and integral gains of IPC changing in the interval [–4e–8,0] rad/(Nm) every 2e–9 rad/(Nm) for the proportional gain k_P and [–4e–8,0] rad/(Nm·sec) every 2e–9 rad/(Nm·sec) for the integral gain k_I. The IPC gain attenuation factor ζ has been set to 0.5 between $U_0 = 10$ m/sec and $U_0 = 12$ m/sec, i.e. in an interval close around the rated speed of $U_{0,r} = 11$ m/sec. These settings have been deemed reasonable after visually checking the time histories in some cases with the proposed boundary values for the gains, measuring the corresponding peak–to–peak amplitude of the pitch signal and monitoring the behavior of torque, rotational speed of the rotor and power output for unacceptably aggressive control performance.

As highlighted in a previous section, IPC receives as input Coleman's transformed measures of blade root bending moments. Blade moments are preliminarily low–pass filtered with a fourth order Butterworth low–pass filter limiting the bandwidth of the signals to the the 1P frequency, in order to avoid spurious contribution from higher harmonics to the transformed loads.

A first analysis is concerned about the effect of weights. It is interesting to check what effect can be obtained with the incremental addition of the various terms in J_c. This can be studied by starting with all–zero weights, then incrementally setting them to non–zero values.

The plots in Fig. 1 have been obtained computing the value of J_c for null weights on all quantities except $g_j = h_j = 10$ (top–left), $l_j = m_j = 10$ (top–right) and $a_j = 0.1$ (bottom–left) respectively. The plot to the bottom–right of the figure has been obtained by superimposing the previous three, i.e. considering a merit function where the weights on blade load peak–to–peak are $g_j = h_j = 10$, those on shaft load average $l_j = m_j = 10$, and that on ADC $a_j = 0.1$. For all these cases the Weibull scaling effect has not been included in the weights, so all weights are the same for all considered wind speeds. The quantity presented in the plots is the relative change of the merit function J_c with respect to the value $J_{c,\mathrm{ref}}$ obtained for $k_I = k_P = 0$, or in analytical terms

$$\delta J_c = \frac{J_c - J_{c,\mathrm{ref}}}{J_{c,\mathrm{ref}}}. \tag{18}$$

By constitution, quantity δJ_c assumes a null value for null IPC gains, i.e. in the reference condition when only the trimmer is controlling the machine. A negative value of δJ_c corresponds to a better performance with respect to the reference, whereas a poorer performance with respect to the reference would result in a positive δJ_c. Consequently, for better clarity, positive values of δJ_c corresponding to an uninteresting performance of the controller are not reported in the plots. The only exception is the bottom–left plot in

Fig. 1, where δJ_c assumes only positive values due to the fact that only ADC has a non–null weight for that case, and such parameter increases proportionally to the intensities of IPC gains.

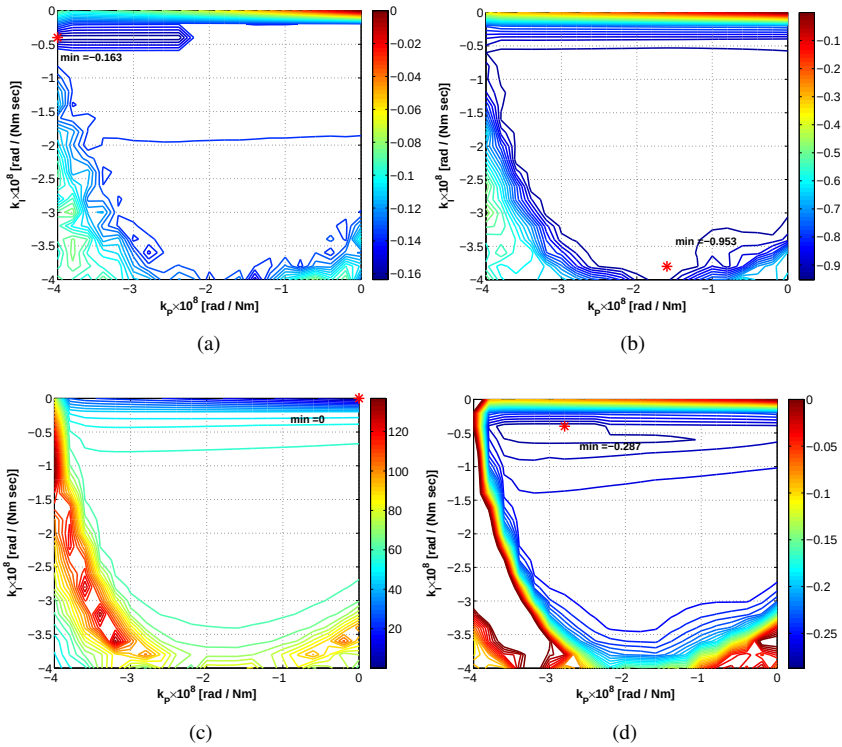

Figure 1. Contour plots of δJ_c as a function of k_P and k_I. Top–left: null weights except $g_j = h_j = 10$. Top–right: null weights except $l_j = m_j = 10$. Bottom–left: null weights except $a_j = 0.1$. Bottom–right: weights $g_j = h_j = l_j = m_j = 10$, $a_j = 0.1$. No Weibull scaling.

A good balance between the components of J_c is confirmed by the right–bottom plot Fig. 1(d), where it is possible to recognize the effect of the three components of J_c (peak–to–peak of blade moments, average of shaft moments and average ADC) selectively weighted in plots (a), (b) and (c).

More in particular, the position of the minimum for higher values of the proportional gain k_P on plot (d) reflects the effect seen on plot (a), and bound to the top reduction of the peak–to–peak of blade loads being obtained for a small range of k_P and and a precise value of k_I. The effects on J_c of the average shaft loads seen on (b) and of ADC presented on (c) are clearly opposed, and together influence the shape of the merit function that can be observed in plot (d). They create a gradient in the direction of k_I that from top of plot (d), i.e. for null k_I, is initially sharply negative for increasing absolute values of k_I, then becoming mildly positive after reaching the minimum of the merit function, up to a

condition where all advantage is lost due to an excessively aggressive control action, and δJ_c returns to zero.

The areas of Fig. 1(d) close to the bottom–left and bottom–right corners, whilst corresponding again to negative values of δJ_c, are not of any practical interest. The relatively low values of J_c in such regions are dictated by a lower ADC component, as can be seen on plot (c), in turn due to the fact that in some simulations IPC is so aggressive that it is deactivated by the control supervisory system, to avoid disturbances to the trimming action and negative consequences to the actuators. In such conditions, only the collective component regulated by the trimmer remains active, thus the corresponding motion of the actuators is limited, causing a lower ADC.

Considering the plot in Fig. 1(d), it can be noticed that for an assigned proportional gain k_P the merit function is gently increasing for a range of values of the integral gain k_I beyond the optimum. On the other hand, it is also noteworthy that a very intense negative gradient shows up in the k_I direction for very small values of k_I (close to the top of the plot), indicating that a good performance advantage can be obtained with a very modest albeit non–null contribution of the integral control component. The effect of the proportional gain k_P on the merit function is generally more limited than that of the integral gain. For a null value of the integral gain k_I (i.e. at the top of the plot) it is possible to observe a negative gradient of J_c for increasing absolute values of the proportional gain k_P, but this gradient is less intense than the aforementioned one in the k_I direction for an assigned k_P. Notwithstanding the generally more reduced effect of proportional control, the position of the minimum of J_c in the case represented on plot (d) is obtained for a non null value of k_P, showing that the contribution of this control component is not negligible, as far as the actual optimal solution is pursued.

As previously pointed out, it should be remarked that an appropriate tuning of the weights should make the merit function depend on all components in such a way as to possibly balance their effects, without any of them overwhelming the others. In particular, as previously reported ADC increases rapidly with higher absolute values of the gains, and increasing a_j to a greater extent than in Fig. 1 leaving the other weights unaltered would result in a merit function totally dominated by the rapid increase of the ADC performance index. This in turn would make this merit function less suitable for an optimal analysis.

In order to provide a more complete picture of the sensitivity of the merit function with respect to the weights, in Fig. 2 some results obtained changing the weights in J_c are presented. Values for the weights considered in Fig. 2 are variations from the reference condition $g_j = h_j = l_j = m_j = 10$ and $a_j = 0.1$. The latter set of weights is the one previously used for the bottom–right plot in Fig. 1, to which the plots in Fig. 2 should be compared. In particular, the plots on the top row refer to weights $g_j = h_j = 5$ to the left and $g_j = h_j = 20$ to the right respectively, leaving all other weights unaltered. Similarly, on the mid row results obtained with weights $l_j = m_j = 5$ to the left and $l_j = m_j = 20$ to the right are reported, whereas on the bottom rows $a_j = 0.05$ and $a_j = 0.2$ have been considered for plots to the left and to the right respectively.

From Fig. 2 it can be observed that, despite an expected intense change in the values assumed by δJ_c in the various proposed cases, the general shape of the merit function

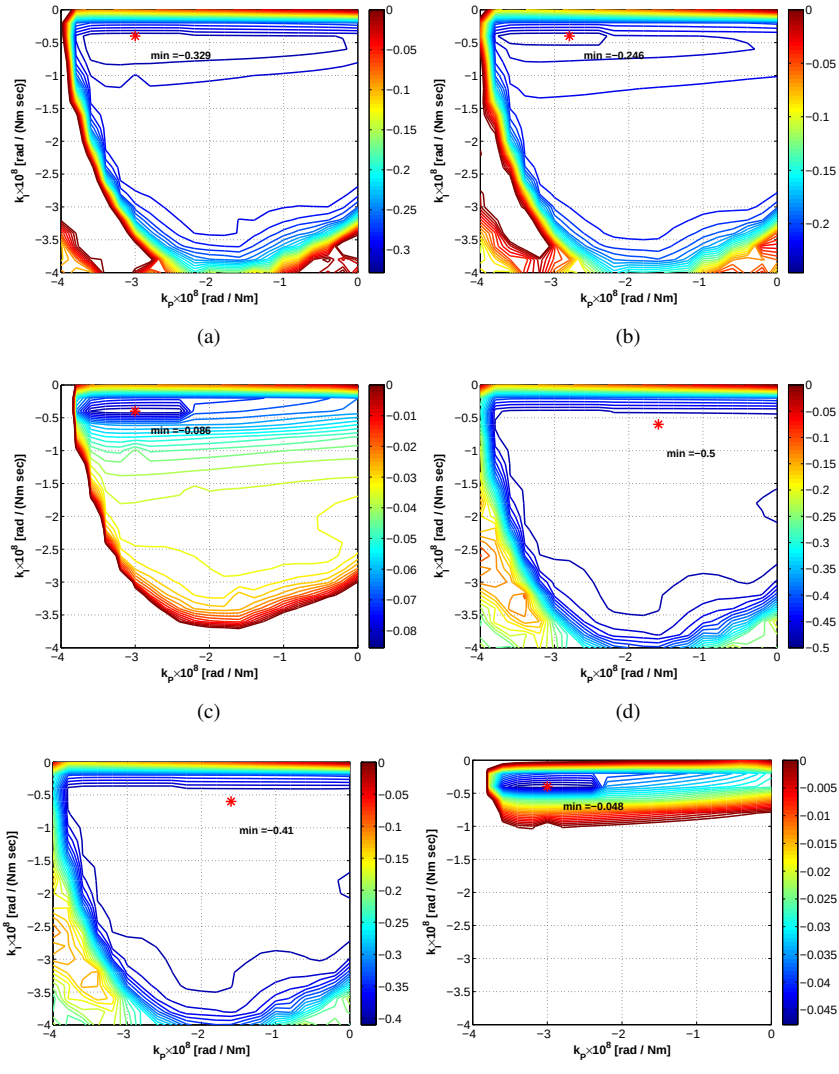

Figure 2. Contour plots of δJ_c as a function of k_P and k_I, showing the effects of changes to the weights. Top plots: changes in g_j and h_j. Mid row: changes in l_j and m_j. Bottom row: changes in a_j. No Weibull scaling.

tends to remain basically unchanged, so the remarks presented for the case for Fig. 1(d) concerning the gradients and the position of the minimum still apply when halving or doubling the weights considered for Fig. 1(d).

More in depth, comparing the results on the top row of Fig. 2 with the plot in Fig. 1(d) it is possible to notice that by upscaling the weights on blade load peak–to–peak, as for plot 2(b), the minimum tends to be located in a slightly more pronounced dip in the merit function, whereas by lowering the same weights the merit function tends to be flatter around the optimum (plot 2(a)). The two plots 2(a) and 2(b) are indeed very similar, as witnessed also by the limited change in the optimal level of δJ_c, indicating a mild impact of the weights of the load peak–to–peak g_j and h_j on the general shape of the merit function, all other weights being equal.

On the other hand, the left plots 2(c) and 2(e) bear a larger difference with respect to the corresponding right plots 2(d) and 2(f) respectively. By inspecting these four plots more accurately and recalling that positive values of δJ_c have not been included, it is possible to notice that 2(c) and 2(f), respectively obtained lowering the weights on shaft average loads and raising the weight on ADC, are clearly similar in shape, both featuring an evident region of optimality for a relatively broad array of values of k_P and a very limited range of values of k_I. Also the plots 2(d) and 2(e), respectively obtained raising the weights on shaft loads and lowering the weight on ADC respectively, are very similar and feature a less pronounced gradient in the k_I direction, and a generally wider region of near–optimality of the merit function.

Notwithstanding their different shapes, the positions of the minima in all plots in Fig. 2 do not change much from one another, especially in terms of the integral gain k_I, and for a range of k_P values roughly between one–third and three–quarters of the top negative gain considered.

Summarizing what has been presented to here, an analysis referring to an ideal constant wind testing scenario shows that, provided the weights are suitably tuned, the selected merit function J_c has a shape such that it can be optimized with respect to the IPC gains k_P and k_I. Furthermore, it is immediately evident that the integral action of the controller is mostly influential when limited but non–null values of the corresponding gain k_I are assumed. On the other hand, even though a certain proportional action is necessary for obtaining the actual minimum of the merit function, the action of the proportional controller is comparatively less pronounced than that of the integral term in lowering J_c.

Turbulent wind scenario For the turbulent wind scenario $N_{U,\,t} = 12$ simulations in IEC Cat. A (IEC61400-1 (2005)) wind with average speeds from $U_{0,\,i} = 3$ m/sec to $U_{0,\,o} = 25$ m/sec every 2 m/sec and a time length of 600 sec have been performed. The same range has been considered for k_P and k_I as for the ideal constant wind case. Also the settings of the gain attenuation factor ζ from the previous scenario have been maintained.

The weights in J_t have been balanced following considerations similar to those illustrated for the constant wind scenario, yielding the set of weights $p_j = q_j = r_j = s_j = 20$, $l_j = m_j = 1$ and $a_j = 0.5$. Interestingly, compared to the weights obtained for balancing the effects of loads and ADC on J_c in the constant wind scenario, the weights on the DEL of the shaft and blade loads need to be higher than those on the peak–to–peak of the blade loads in the constant wind case. This suggests that the effect of IPC on the DEL in turbulence is less marked than that on the peak–to–peak in constant wind. On

the other hand, the balance between ADC and shaft average loads indicates a generally greater effectiveness of IPC on these loads when compared to the constant wind case.

In Fig. 3 the results obtained in the turbulent scenario on the merit function J_t are presented. To the left the weights $p_j = q_j = r_j = s_j = 20$, $l_j = m_j = 1$ and $a_j = 0.5$ have been considered, whereas in the plot to the right the same weights have been used as starting values and multiplied by the appropriate value of the IEC (IEC61400-1 (2005)) Weibull function for the corresponding average wind speeds as in Eq. 17, yielding different weights for simulations at different wind speeds. The quantity δJ_t, formally defined as δJ_c in Eq. 18 changing J_c with J_t, is considered in both plots in Fig. 3. Similarly to δJ_c, only negative values of δJ_t are considered for the plot, positive values being representative of an uninteresting, detrimental control performance.

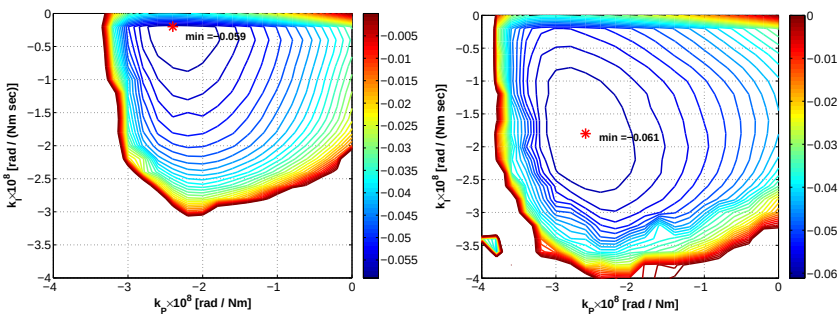

(a) (b)

Figure 3. Contour plot of δJ_t as a function of k_P and k_I. Left: no Weibull scaling of weights. Right: all weights scaled with Weibull function based on the corresponding average wind speed. Non–null weights on time average of shaft loads, DEL of blade and shaft loads, and ADC.

From the left plot in Fig. 3 it is possible to notice that the result on J_t in turbulent wind is not far from that in Fig. 1(d) in terms of general shape, of the direction and intensities of the gradients and of the location of the minimum. This very relevant fact stands in support of a gain tuning procedure based only on the use of less computationally heavy constant wind simulations, without involving the more complicated and time–consuming turbulent wind scenario in the analysis. Similarly to the constant wind scenario, the gradient in the k_I direction is very intensely negative for an assigned intermediate value of k_P and a low absolute value of k_I, and comparatively mildly positive for increasing absolute values of k_I beyond the optimum. This suggests that the level of J_t can be maintained close to the optimum in terms of k_I for a range of integral gains, but a non–null value of this gain is necessary to get a good performance. As for the constant wind scenario, the gradient in the k_P direction is less marked than in the k_I direction, but the optimum is clearly characterized by a non–null proportional gain, in a range between the half and three–quarters of the absolute value of the top negative gain considered in the analysis.

The plot to the right of Fig. 3 is based on the same simulation results considered for the plot to the left, but the weights for each simulation are scaled with respect to their respective average speed according to Eq. 17. The effect is mainly that of shifting the position of the near–optimality region, especially increasing the value of k_I corresponding to the optimum. The intensity and location of the gradients in the k_P direction compare well with those on the left plot on Fig. 3, as well as the position of the optimum in terms of k_P.

It is noteworthy that a procedure for optimal gain selection based on the merit function J_t may have different solutions in terms of k_P and k_I in the proposed turbulent scenario in case the Weibull distribution were taken into account or not, but due to the moderated gradient of the merit function in both cases along the directions of both k_P and k_I in a region surrounding the minimum of J_t, the difference in the level of optimality for the optimal and a near–optimal combination of the gains shall be very limited. In other words, an optimal solution for one of the two problems will be near–optimal also for the other. Despite the similarity in the shapes of the two merit functions close to the respective optima in the two plots on Fig. 3, assuming to remove the Weibull weighting would be advisable for a preliminary assessment of control performance, whereas for an evaluation of the overall performance of the controller over the lifespan of the turbine such scaling should be accounted for. In this fashion, comparing the two plots in Fig. 3 it is possible to argue that a more intense value of k_I, which as previously pointed out appears to be needed for keeping the control solution to the optimum when considering the Weibull scaling, plays an important role when considering the lifespan of the turbine, whereas a more limited but non–null k_I together with a proportional action would suffice when not accounting for long term effects.

As a closing consideration, it can be noted that the results obtained in this section are largely in accordance with the theory of IPC, for which the integral control component has a primary relevance in the performance of this control layer, whereas the effect of proportional control should be in principle unnecessary. Such theory is developed for an ideal system in strictly time–periodic conditions, but the results presented here for more realistic constant and turbulent wind scenarios, working on a sophisticated model of a real machine, tend to confirm its predictions (Bossanyi (2004); van Engelen and Kanev (2009); Riboldi (2012); Bottasso et al. (2013)).

Effect of conditional activation

An alternative to the use of IPC over the full span of wind speeds between cut–in and cut–out is proposed in Bottasso et al. (2014), showing potentially interesting results on the envelope of the machine when selectively activating IPC only for some wind speeds. In the proposed reference much attention was devoted to maximizing the effect of IPC on some ultimate loads top–scoring in the ranking of loads for the considered machine. The selection of the activation range in the scope of that analysis was basically a matter of hand tuning.

In the current analysis the merit function J_t provides a measure of the performance of IPC comprising both the advantageous effects on loads and detrimental effects on

ADC, hence the effect of the amplitude of the activation range can be studied through the analysis of J_t.

As for the case of gains, one of the objectives of the present analysis is that of favoring a visual perception of the shape of the merit function. For this reason, in order to study the effects of conditional activation on J_t, only the two amplitudes R_r and R_o of the activation ranges have been considered as tuning parameters, respectively centered at the rated wind speed minus 2 m/sec, $U_{0,\,r-2} = 9$ m/sec, and cut–out wind speed $U_{0,\,o} = 25$ m/sec. The choice of the values of the focal speeds was driven by the already mentioned analysis in Bottasso et al. (2014), and is bound to the relevance of these particular speeds on the load envelope and ranking of a typical three–bladed horizontal axis wind turbine of multi–MW size. The rated minus 2 m/sec has been preferred to the rated in order to avoid overlapping of the activation ranges, thus easing the analysis of the results without altering the meaning of the theoretical effects of the parameters. The gains of IPC have been frozen at the values representing the optimal condition according to the analysis in the turbulent scenario proposed previously in this section, visually presented to the right of Fig. 3, with $k_P = -2.72e-8$ rad/(Nm) and $k_I = -1.8e-8$ rad/(Nm·sec) for proportional and integral gains respectively. The setting of the attenuation factor ζ have been left unaltered with respect to the previous scenarios. The values of range considered in the analysis are in [0, 16] m/sec every 2 m/sec for both R_r and R_o. Recalling Eq. 7 it can be noticed that with this choice of values the two operational regions never overlap.

As explained in a previous section, the control logic for activating and deactivating the IPC when entering or leaving an operational region is also responsible for smoothing the transition between the on and off conditions of this control layer. The activation/deactivation procedure is triggered based on a moving–average filtered value of the wind speed measured on top of the tower, the filter having a characteristic time of 10 sec. The transition maneuver for IPC activation or deactivation takes a time of 5 sec to complete.

Figure 4 shows the behavior of δJ_t with the same weights used for the results in Fig. 3 ($p_j = q_j = r_j = s_j = 20$, $l_j = m_j = 1$ and $a_j = 0.5$), when considering the Weibull scaling (right) or not (left).

Considering both plots, it is immediately apparent that the effect of the cut–out range R_o is more visible when the Weibull is not accounted for (left plot). This is in accordance with the great effectiveness of IPC for higher values of the wind speed, which is reflected in relevant advantages on loads, in accordance with the literature (Riboldi (2012); Bottasso et al. (2013)). The Weibull scaling significantly reduces the importance of the high wind speed region, hence lowering the effect of parameter R_o with respect to R_r.

From both plots in Fig. 4 it can be noticed that the merit function is lower for higher values of both ranges, with the optimum reached for top values of both R_r and R_o. The actual optimal solution in the scenario considered for Fig. 4 lies very close to the top bounds of R_r and R_o, corresponding to the activation of IPC over all the operating regions of the machine.

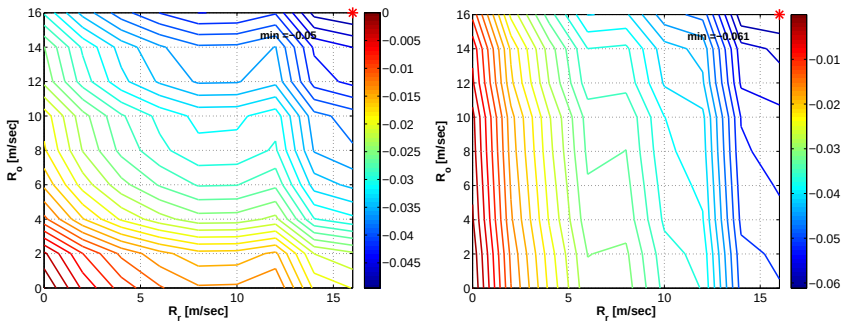

Figure 4. Contour plots of δJ_t as a function of R_r and R_o. Left: no Weibull scaling of weights. Right: all weights scaled with Weibull function based on the corresponding average wind speed.

On the other hand, looking more carefully at the plot to the right, it can be noticed that the level of J_t changes only slightly in a rectangular region extending from $R_r = 14$ m/sec to $R_r = 16$ m/sec, and for all values of R_o. The difference between the maximum and minimum values of δJ_t in this region is $\delta J_t(14, 0) - \delta J_t(16, 16) = -0.0115$, where the value of δJ_t corresponding to the optimum is $\delta J_t^{\text{opt}} = \delta J_t(16, 16) = -0.0612$. The ratio between the two is 18.8%, representing the top performance improvement that can be obtained in the selected rectangular area. For comparison, the value of δJ_t for $R_r = 14$ m/sec and $R_o = 0$ m/sec (on the lower boundary of the plot), corresponding to the difference between $\delta J_t(14, 0)$ and $\delta J_t(0, 0)$ (recall the definition of δJ_t for which when $R_r = R_o = 0$ m/sec then $\delta J_t = 0$, i.e. IPC is not working), is $\delta J_t(14, 0) = -0.0497$, and the ratio of this value over δJ_t^{opt} is correspondingly 81.2%. This represents the top improvement that can be obtained with an IPC action only around $U_{0,r-2}$ with an operative range of $R_r = 14$ m/sec. It can be noticed that the latter difference is by far more significant than the former, confirming the little relevance of R_o in optimizing the performance.

The results in Fig. 4 clearly show that testing the effect of gains considering the Weibull or not may alter the tuning procedure of the control system, making some design parameters almost irrelevant. As previously commented, even though not including the Weibull may be acceptable for a preliminary analysis, this is not the case for a more design–oriented analysis, accounting for the performance of the machine over the intended lifespan. According to this consideration the scenario corresponding to the right of Fig. 4 would be more relevant, and this in turn would reduce the importance of R_o in the computation of the optimal tuning condition.

The shape of the merit function remains basically similar to that shown in Fig. 4 also altering the values assumed for k_P and k_I in the optimal region shown on the plot to the right of Fig. 3. On the other hand, altering the weights in J_t may produce some changes

to the merit function. As an example, in Fig. 5 the map of δJ_t with respect to R_r and R_o is presented for two sets of Weibull–scaled weights, where the starting value of the weights is the same as for Fig. 4 except for a_j, which has been obtained starting from doubled and halved $a_j^* = 1$ and $a_j^* = 0.25$ respectively in the plots to the left and to the right. The same optimal values of the gains considered for Fig. 4 have been considered also here.

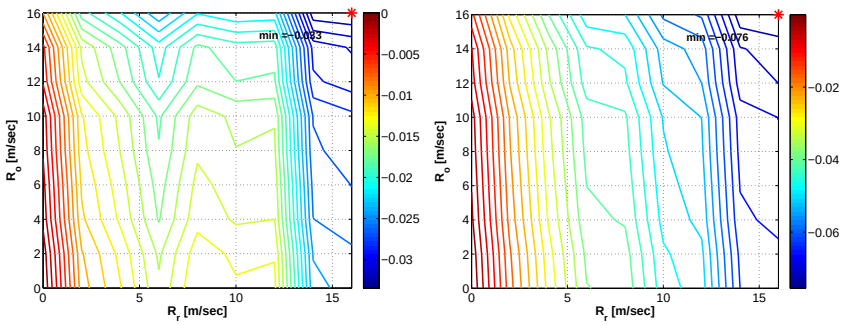

(a) (b)

Figure 5. Contour plots of δJ_t as a function of R_r and R_o. All weights scaled with Weibull function based on the corresponding average wind speed. Starting weights as in Fig. 4 except $a_j^* = 1$ (left) and $a_j^* = 0.25$ (right).

From Fig. 5 it can be seen that when doubling the weight on ADC (left) a region of local minimum appears in the shape of the merit function around $R_r = 6$ m/sec and $R_o = 16$ m/sec. The absolute optimum remains close to the top values of R_r and R_o, i.e. for the IPC working at every wind speed. Considering $R_r = 6$ m/sec and $R_o = 0$ m/sec, the gain with respect to what is obtained with an only collective controller ($R_r = R_o = 0$ m/sec) is 45.8% of the optimum δJ_t^{opt}. This result shows that a higher weight on ADC, meaning a greater relevance of actuator strain in the computation of the overall performance, generates a scenario where roughly half of the global performance is obtained by using IPC only in a limited region close around the rated wind speed.

On the other hand, the result obtained lowering the weight on ADC (right plot on Fig. 5) is very similar to that previously shown to the right of Fig. 4, which was the result of the same balance between all terms in J_t considered when studying the effects of gains in the previous section.

Optimization results

As previously explained, the mapping of the merit function has been carried out also in order to privilege a visual understanding of the behavior of J_c and J_t with respect to the control design parameters. For this reason, the effect of two parameters at a time has been considered.

The results presented above suggest a greater influence of k_I with respect to k_P considering J_c in an ideal scenario and J_t in a turbulent scenario respectively, whereas R_r is more influential than R_o on J_t in turbulent wind, especially when considering the Weibull distribution for scaling the weights. The latter scenario is probably the one of greatest interest from the viewpoint of industry, due to the greater realism of turbulent simulations with respect to constant wind simulations, and to the fact the Weibull probability distribution is usually accounted for in the design process whenever results scattered over the wind speeds for which the machine is designed are taken into account (IEC61400-1 (2005)).

Considering the turbulent scenario and J_t, in the previous sections optimal solutions have been explored visually for two separate optimization problems, where the dependence of the merit function has been considered on the couples k_P, k_I and subsequently R_r and R_o.

In this section some results from numerical optimization runs are presented. The motivations for performing such further analyses are basically two. Firstly, in order to assess the correctness and level of precision of the results visually presented above for the two optimal problems just mentioned. Secondarily, in order to quantify the difference of the optimal solutions found from such partial analyses and more complete optimization problems where all control design parameters are considered together.

When more than two optimization variables are considered simultaneously it is not possible to visually check the behavior of the merit function, thus making considerations like those presented above more difficult. On the other hand, a more complete optimization problem based on more than two parameters will probably bear a solution in terms of gains and ranges different from that obtained by solving the two aforementioned optimizations separately. The only way to check the consistency of the optimal solutions in all such cases is by numerically optimizing the merit function and compare results.

As highlighted through the results previously presented, the shape of J_t with an appropriate choice of weights is suitable for a numerical optimization. Moreover, as the merit function appears to be a regular function of the two considered sets of parameters (two gains and two activation ranges), the respective optimizations can be safely run with a state–of–the–art SQP gradient–based algorithm. For the optimization problems for which the shape of J_t cannot be visually investigated a priori, a genetic algorithm has been used, in order to reduce the chance of selecting a solution corresponding to a potential local minimum. In that case, a population of twenty individuals has been considered, compliant with the specified optimization bounds.

For all problems, the convergence tolerance on the merit function for the numerical optimization method has been set to 10^{-4}. The optimization problems are unconstrained, with bounds on the optimization variables. Whenever considered, k_P and k_I are bound to the interval [–4e–8,0] rad/(Nm) and rad/(Nm·sec) respectively, whereas R_r and R_o are bound to the interval [0,16] m/sec. The focal speeds for the activation range has been specified similarly to the previous sections as $U_{0,\,r-2} = 9$ m/sec and $U_{0,\,o} = 25$ m/sec respectively for R_r and R_o.

The adopted cost function J_t has been computed based on starting weights $p_j^* = q_j^* = r_j^* = s_j^* = 20$, $l_j^* = m_j^* = 1$ and $a_j^* = 0.5$. These have been scaled according to

the Weibull probability function depending on the average wind speed (IEC61400-1 (2005)). The same $N_{U,\,t} = 12$ simulations of 600 sec in Cat. A turubulence proposed in the previous sections have been considered.

The results of the optimizations are reported on Tab. 1. The values specified for active parameters have been computed through a numerical algorithm as a solution of the optimal problem, whereas those associated to non–active parameters have been specified as fixed data in the computation of the optimal solution. Cases n. 1 to 3 refer to optimal problems of the same quality of those treated in the previous sections, where J_t has been analyzed as a function of two parameters at a time. In particular, case n. 1 refers to the same condition treated in Fig. 3, whereas cases n. 2 and 3 refer to that treated in Fig. 4. Solutions for these optimization problems have been obtained with a gradient–based algorithm. Cases n. 4 and 5 refer to optimization problems with more than two parameters, and these have been solved with a genetic algorithm as previously explained.

Case Id.	k_P		k_I		R_r		R_o		δJ_t^{opt}
	Active	Value	Active	Value	Active	Value	Active	Value	
1	yes	$-2.72e{-8}$	yes	$-1.80e{-8}$	no	16.0	no	16.0	-0.0612
2	no	$-2.72e{-8}$	no	$-1.80e{-8}$	yes	15.5	yes	15.7	-0.0617
3	no	$-2.72e{-8}$	no	$-1.80e{-8}$	yes	15.33	no	0	-0.0511
4	yes	$-2.77e{-8}$	yes	$-2.38e{-8}$	yes	15.4	no	0	-0.0516
5	yes	$-2.73e{-8}$	yes	$-1.83e{-8}$	yes	15.6	yes	15.7	-0.0618

Table 1. Results of optimizations. Active parameters for optimization as specified. Values reported for non–optimized parameters have been specified in the optimization routines. Values reported for optimized parameters have been computed as optimal values by the optimizer. Optimal values of δJ_t^{opt} computed accounting for Weibull weighting. Upper section: solution through gradient–based algorithm. Lower section: solution through genetic algorithm.

The first two cases in Tab. 1 confirm the results obtained in the previous subsections. Actually, the optimal values of the gains obtained for case n. 1 have been used for obtaining the map in Fig. 4. The result of case n. 2 shows a negligible difference with respect to n. 1 on the active parameters R_r and R_o. The limited improvement in the level of optimality that apparently can be obtained by slightly reducing the activation ranges of IPC is probably due to the adopted simulation grid, and running multiple simulations with various turbulence seeds would likely push the optimal solution towards a condition corresponding to a full–span activation, in accordance with what has been visually found in Fig. 4.

Case n. 3 has been implemented in order to check the change of the optimality level when R_o is not considered as a parameter for optimization. Considering cases n. 2 and 3 together it can be seen that a limited percent rise in δJ_t^{opt} of about 17.1% is obtained by inhibiting IPC around the cut–out, in practice reducing it drastically from $R_o = 15.7$ to $R_o = 0$ m/sec. This shows that, as preventively assessed in the previous analyses, R_o is not a critically relevant control design parameter as far as Weibull scaling is considered, being responsible for less than one–fifth of the overall performance improvement.

Generally speaking, the results of cases n. 1, 2 and 3 tend to confirm the validity of the observations presented commenting the results of the previous sections (Fig. 3 and 4).

From the analysis of the results of cases n. 4 and 5 it is apparent that a numerical optimization simultaneously accounting for more than two parameters does not provide significant advantages in terms of change to the optimal value of J_t^{opt} with respect to the corresponding sub–problems. The values of the optimal gains are not much different from those obtained from case n. 1. Furthermore, considering the most general case n. 5 the values of the ranges are not far from those obtained for case n. 2, whereas the value for the optimal R_r in case n. 4 is close to that found in the similar case n. 3. Once more, comparing the value of δJ_t^{opt} for cases n. 4 and 5, a loss of performance δJ^{opt} of about 16.5% is obtained when dropping parameters R_o from the optimization problem. As discussed above for cases n. 2 and 3, this means that by reducing $R_o = 15.7$ m/sec to $R_o = 0$ m/sec, and slightly adjusting the other free optimization parameters, a relatively small loss on optimality is obtained, limited under one–fifth of the best performance, hence confirming a light effect of R_o in the considered optimization problem.

Comparing results in Tab. 1, it appears that the solution of the optimization problem over four parameters can be split into two separate sub–problems without significant losses in the level of optimality, i.e. in the value J_t^{opt} and consequently δJ_t^{opt}. This further justifies the approach by sub–problems proposed in this paper, which is not only advantageous for getting a visual understanding of the behavior of the merit function and of the significance of the various terms in it, but also allows to effectively seek for an optimal condition which is very close to the actual optimal condition found solving a more complete optimization problem.

This notion can be effectively exploited for reducing the computational effort required for tuning. All gradient–based optimization (cases n. 1 to 3) have been completed with a convergence tolerance of 10^{-4} on J_t with a number of evaluations of the merit functions in the range of 30 to 50. Genetic algorithms applied to this optimization problem (cases n.4 and 5) with the same tolerance (10^{-4}) on the difference between the scores of individuals and a population of 20 individuals for each generation can easily require 700 to 900 evaluations. The latter figures should be taken with caution, for as this research demonstrated the actual position of the optimum for J_t as a function of more than two parameters does not fall far from the respective optima obtained for partial problems based on two parameters, hence the initial population has been selected accurately close to the most likely position of the optimum, thus possibly easing convergence. On the other hand, even though the position of the actual optimum of the merit function is not altered by a change in the weights, some form of dependence on their values does exist in the considered scenario, as shown for instance in Fig. 5. Further changes to the weights, possibly due to particular design necessities aimed at penalizing some terms most, may alter the shape of the function more markedly, potentially causing the need to increase the size and scatter of the initial population of a genetic algorithm in order to safely avoid local minima. However, in case the problem of optimality based on all parameters can be split into two sub–problems, it would be possible to safely switch from a genetic algorithm to a gradient–based one, with a great saving on computational time.

Conclusions

The focus of the research presented in this paper was that of studying the feasibility of an optimal tuning procedure for an individual pitch control (IPC) law to be applied to horizontal axis wind turbines, and consequently of understanding how to set up such procedure.

To this aim a realistic architecture of an IPC control law was proposed and implemented. The parameters of interest for the tuning process have been defined as the proportional and integral gains of the IPC law, as well as the extensions of the two IPC operational ranges centered at two different wind speeds.

Two operational scenarios have been considered for studying the performance of the controller for different values of the tuning parameters, an ideal constant wind scenario and a turbulent wind scenario. Performance indices measuring the positive effects on loads and the detrimental effects on pitch actuator strain have been defined and assembled in merit functions suitable for an optimality study.

The importance of the weighting process for both the ideal and turbulent wind scenarios has been investigated. In particular, it was shown that normalized changes in actuator duty cycle (ADC) should be accompanied by a relatively low weight in the merit function, due to their naturally greater intensity with respect to load performance indices. This in spite of the great relevance ADC generally has for industrial subjects. Failing to suitably balance weights may result in a merit function not featuring an optimum within the assigned bounds of the optimization parameters. Such bounds have a physical meaning. For the case of gains, they have been chosen in order to avoid an excessively intense or fast action of IPC, resulting in a poor control action due also the filtering action of pitch control commands by the dynamics of pitch actuators, and possibly such to force the control supervisor to intervene shutting–off the turbine. For the case of activation ranges, focal speeds and bounds are designed to cover the whole operating range of the turbine when both range values are at their top limits, whilst avoiding any overlap.

In order to privilege a visual analysis of the results, the proposed merit functions have been mapped with respect to two parameters at a time at most. The analysis as it was configured with respect to two scalar gains and two amplitudes of the corresponding operational ranges is suitable for a similar mapping.

The dependence of the merit function on IPC gains has been investigated, showing that notwithstanding a certain dependence of the specific optimal gain set on the weights, the solution tends to be similar for both the ideal and turbulent scenarios, and for the latter either accounting for a Weibull distribution in the weights or not. The optimal solution is characterized by a non–null but comparatively small value of the integral gain, and by a value of the proportional gain in a range between the half and three–quarters of the absolute value of the top negative gain considered for the investigation. A limited shift of the optimum towards a more intense integral gain can be observed when including the Weibull weighting in the turbulent scenario. This comes together with less pronounced intensities of the gradients in the directions of the proportional and integral gains around the optimum, implying that near–optimal solutions in a limited but visible area around the optimum be not far from it.

This provides a very strong indication, suggesting that the need for considering the more time consuming and complicated turbulent scenario for tuning the IPC gains is not stringent. Put another way, optimal tuning of the gains may be carried out in the ideal constant wind scenario, the result being nearly optimal also in turbulent wind.

The dependence of the merit function on the operational ranges has been analyzed for the turbulent scenario. Differently from the analysis with respect to IPC gains, the effect of ADC weighting is here less pronounced, whereas the choice of including the Weibull scaling in the weights plays a relevant role. When the Weibull scaling is not considered the merit function is greatly reduced by increasing the width of the operational range around the cut–out speed, with the size of the range around the rated being as much important. When the Weibull scaling is accounted for, the roles played by the amplitudes of both ranges are more different, with R_o being almost uninfluential. This is in accordance with the fact that, when considering the Weibull, the high speed operational range where substantial advantages on loads are obtained with IPC is less relevant to the global performance.

This shows that accounting for the Weibull scaling or not may imply a simplification in the tuning, as far as these performance indices are considered. In case the Weibull function is accepted to be reflecting a realistic distribution of the wind speed, or when dictated by industrial needs in turn stemming from standard requirements, it should be accounted for. If the Weibull is accounted for, parameter R_o is not very influential and can be excluded from the tuning procedure.

In order to check the reliability of the results obtained considering partial sets of design parameters and to better assess the influence of the various parameters on the quality of the optimal solution, some full numerical optimizations have been carried out in the more realistic turbulent scenario. The same Weibull–scaled weights have been considered for all optimizations, whereas different choices of optimization parameters have been considered. The results of the optimizations have confirmed that considering different sets of parameters does not alter significantly neither the optimal value of the merit function nor the corresponding values attributed to the various considered parameters for each case, which are sometimes only slightly different.

The results of optimizations highlight two important facts concerning tuning. Firstly, the little impact of parameter R_o on the level of the optimal solution in the adopted test scenario is remarked once more. Secondarily, the level of the optima attained solving the partial optimizations over two parameters (gains or operational ranges) are very similar to those obtained solving the optimal problems based on larger parameter sets. This implies that the optimizations of the gains and of the ranges can be carried out as separate processes whenever needed, with a great saving in computational effort and execution time.

Acknowledgements

The contribution of Federico Gualdoni, Ph.D. and Riccardo Riva, M.o.S. in the setup of the analysis and in the discussion of the results is gratefully acknowledged. The computations instrumental

in the production of this work have been carried out with the computational resources of the Department of Aerospace Science and Technology, Politecnico di Milano.

Declaration of conflicting interests

The Author declares that there is no conflict of interest.

Funding

This research received no specific grant from any funding agency in the public, commercial, or not–for–profit sectors.

References

Bauchau OA, Bottasso CL and Trainelli L (2003) Robust integration schemes for flexible multibody systems *Computer Methods in Applied Mechanics and Engineering* 192: 395–420.

Bossanyi E (2003a) Wind turbine control for load reduction *Wind Energy* 6: 229–244.

Bossanyi E (2003b) Individual blade pitch control for load reduction *Wind Energy* 6: 119–128.

Bossanyi E (2004) Developments in individual blade pitch control. In: *Proceedings of The Science of Making Torque from Wind Conference*, Delft, The Netherlands, 19–21 April 2004.

Bossanyi E (2005) Further load reductions with individual pitch control *Wind Energy* 8: 481–485.

Bottasso CL and Croce A (2006–2012) `Cp-Lambda`: user's manual. Report, Dipartimento di Ingegneria Aerospaziale, Politecnico di Milano, Italy.

Bottasso CL, Croce A, Riboldi CED and Nam Y (2012) Power curve tracking in the presence of a tip speed constraint *Renewable Energy* 40: 1–12.

Bottasso CL, Croce A, Riboldi CED and Nam Y (2013) Multi–layer control architecture for the reduction of deterministic and non–deterministic loads on wind turbines *Renewable Energy* 51: 159–169.

Bottasso CL, Croce A, Riboldi CED and Salvetti M (2014) Cyclic pitch control for the reduction of ultimate loads on wind turbines *Journal Of Physics Conference Series* 524(1):012063.

Bottasso CL, Croce A, Savini B, Sirchi W and Trainelli L (2005) Aero–servo elastic modeling and control of wind turbines using finite–element multibody procedures. In: *Proceedings of the ECCOMAS Multibody Dynamics 2005 Thematic Conference*, Madrid, Spain, 21–24 June 2005.

Geyler M and Caselitz P (2007) Individual blade pitch control design for load reduction on large wind turbines. In: *Proceedings of the European Wind Energy Conference (EWEC 2007)*, Milano, Italy, 7–10 May 2007.

Geyler M and Caselitz P (2008) Robust multivariable pitch control design for load reduction on large wind turbines *Journal of Solar Energy Engineering* 130:031014/1–031014/12.

IEC61400–1 (2005) Wind turbines – Part 1: design requirements.

Jonkman JM and Buhl M (2005) `FAST` User's Guide. Report, National Renewable Energy Laboratory, Boulder, CO.

Leithead WE, Neilson V and Dominguez S (2009) Alleviation of unbalanced rotor loads by single blade controllers. In: *Proceedings of the European Wind Energy Conference (EWEC 2009)*, Marseille, France, 16–19 March 2009.

Riboldi CED (2012), Advanced control laws for variable speed wind turbines and supporting enabling technologies. PhD Thesis, Department of Aerospace Science and Technology, Politecnico di Milano, Italy. Available at: https://www.politesi.polimi.it.

Stol KA (2003) Disturbance tracking control and blade load mitigation for variable–speed wind turbines *ASME Journal of Solar Energy Engineering* 125: 396–401.

Stol KA and Balas MJ (2003) Periodic disturbance accommodating control for speed regulation of wind turbines *ASME Journal of Solar Energy Engineering* 125: 379–385.

Van Engelen TG (2006) Design model and load reduction assessment for multi–rotational mode individual pitch control (Higher Harmonics Control). In: *Proceedings of the European Wind Energy Conference (EWEC 2006)*, Athens, Greece, 27 February–2 March 2006.

Van Engelen TG and Kanev S (2009) Exploring the limits in individual pitch control. In: *Proceedings of the European Wind Energy Conference (EWEC 2009)*, Marseille, France, 16–19 March 2009.